Observation of large nonlinear responses in a graphene-Bi_2Te_3 heterostructure at a telecommunication wavelength

Yingwei Wang,[1] Haoran Mu,[2] Xiaohong Li,[1] Jian Yuan,[2] Jiazhang Chen,[1] Si Xiao,[1,a)] Qiaoliang Bao,[2] Yongli Gao,[1,3] and Jun He[1,b)]

[1]*School of Physics and Electronics, Hunan Key Laboratory for Super-microstructure and Ultrafast Process, Central South University, 932 South Lushan Road, Changsha, Hunan 410083, People's Republic of China*
[2]*Institute of Functional Nano and Soft Materials (FUNSOM), Jiangsu Key Laboratory for Carbon-Based Functional Materials and Devices, and Collaborative Innovation Center of Suzhou Nano Science and Technology, Soochow University, Suzhou 215123, People's Republic of China*
[3]*Department of Physics and Astronomy, University of Rochester, Rochester, New York 14627, USA*

(Received 18 April 2016; accepted 18 May 2016; published online 31 May 2016)

We report the large nonlinear response and ultrafast carrier relaxation dynamics of a graphene-Bi_2Te_3 heterostructure produced by two-step chemical vapour deposition. The nonlinear refractive index reaches $n_2 = 0.2 \times 10^{-7}\,cm^2/W$ at the telecommunication wavelength of 1550 nm, which is almost seven orders of magnitude larger than that of the bulk Si material. Additionally, a pump-probe experiment is performed to investigate the ultrafast dynamic process (intraband relaxation time $\tau_1 = 270 \pm 20$ fs; interband relaxation time $\tau_2 = 3.6 \pm 0.2$ ps) of the graphene-Bi_2Te_3 heterostructure. Then, based on the donor-acceptor structure model, we propose a theoretical model to explain the dynamic relaxation process. Our results show that the graphene-Bi_2Te_3 heterostructure is a promising saturable absorber for ultrafast pulse laser applications at telecommunication wavelengths. *Published by AIP Publishing.* [http://dx.doi.org/10.1063/1.4953072]

Two-dimensional (2D) materials, such as graphene,[1,2] transition metal dichalcogenides (TMDs),[3,4] and topological insulators,[5,6] have attracted great interest owing to their excellent optical and electronic properties. Currently, there arises a new type of 2D nonlinear optical material, that is, black phosphorus (BP). It shows fascinating nonlinear response,[7–10] broadband saturable absorption, and ultrafast carrier recovery time, which indicate that black phosphorus is a promising material as an effective saturable absorber for pulsed fiber or solid-state lasers, while the rapid surface degradation always hinders its practical application in photoelectric. In recent years, researchers have focused on the 2D heterostructure to improve the characteristics of pure 2D materials. The most intriguing aspect of 2D materials is that new 2D heterostructures materials can be created by stacking different 2D crystals without the conventional "lattice mismatch" issue.

Graphene, a representative 2D crystal material, has been demonstrated to possess outstanding nonlinear and ultrafast dynamic response. In 2012, Zhang *et al.*[11] unambiguously distinguished the saturated absorption and nonlinear refraction of graphene and obtained a nonlinear refractive index of $n_2 \approx 10^{-7}\,cm^2/W$. These properties are suitable for many important applications in photonics and optoelectronics. George *et al.*[12] studied photoexcited carrier ultrafast relaxation and recombination dynamic processes in graphene materials by ultrafast optical-pump terahertz-probe spectroscopy. They suggested that graphene material has ultrafast electron-hole recombination times (thermalizes and cools 10–150 fs, carrier cooling 150 fs–1 ps, and carrier recombination 1 ps–15 ps), and the ultrafast carrier recombination processes provided a possibility for the realization of an ultrashort pulse laser.[13] Based on the excellent nonlinear optical effect of graphene, different applications have been proposed to design Q-switched and mode-locked pulses in fibre lasers, solid-state lasers, and waveguide lasers.[14–17] Nevertheless, the graphene-based lasers face a tremendous obstacle to their practical application because the absolute optical modulation depth of monolayer graphene is very low (approximately 1%).[18] Other 2D nanomaterials known as topological insulators might compensate for this disadvantage. The graphene-Bi_2Te_3 heterostructure possesses much higher modulation depth than that of monolayer graphene, as shown in our previous work.[6] The growth of the graphene-Bi_2Te_3 heterostructure is controllable. It results in that the tunable linear and nonlinear optical properties can be achieved, which has unique advantages and is importantly different from pure graphene and Bi_2Te_3.

Topological insulators are unique because their bulk materials have insulation states, whereas conducting states exist on the edge or surface. Thus, these materials constitute a research focus in the field of condensed matter physics.[19,20] Similar to graphene, the topological insulators have potential as saturable absorbers for pulsed laser applications[21–26] because of their excellent nonlinear optical effects and ultrafast dynamic processes. Chen *et al.*[27] found that Bi_2Te_3 also showed a saturation intensity of $\sim 12\,\mu W/cm^2$ and a normalized modulation depth of ~70% by studying its nonlinear response in the microwave band. Thus, this material has potential photonic applications in both the optical and microwave bands. Hajlaoui *et al.*[28,29] studied the ultrafast evolution of the surface electronic structure of the topological insulator Bi_2Te_3 by time-resolved ultrafast angle-resolved photoelectron spectroscopy excitation. Their results demonstrated that the interband scattering from the bulk conduction band, lasting between approximately 0.5 ps and a few

a)Electronic mail: sixiao@csu.edu.cn.
b)Electronic mail: junhe@csu.edu.cn.

picoseconds, was necessary for the Dirac cone non-equilibrium electrons to recover a Fermi-Dirac distribution. In previous works, the integration of graphene with a topological insulator was explored on its preparation[6,30] and the application of photodetectors.[31] However, few studies have addressed the basic nonlinear optical index and ultrafast dynamics of the graphene-Bi_2Te_3 heterostructure.

In this work, we focus on the basic nonlinear optical response and ultrafast dynamics of the graphene-Bi_2Te_3 heterostructure. Herein, the Kerr-type nonlinearity of the graphene-Bi_2Te_3 heterostructure, which manifests as nonlinear absorption and nonlinear refraction, is observed. The graphene-Bi_2Te_3 heterostructure possesses a large nonlinear refractive index $n_2 = 0.2 \times 10^{-7}\,cm^2/W$. The pump-probe measurements were performed to determine the ultrafast dynamic relaxation process time ($\tau_1 = 270 \pm 20$ fs; $\tau_2 = 3.6 \pm 0.2$ ps), which was observed to longer than that of few-layer graphene but shorter than that of Bi_2Te_3. Subsequently, based on the donor-acceptor structure model, we proposed a possible theoretical explanation for the relaxation process of the heterostructure. The excellent saturable absorption characteristics and ultrafast dynamics recovery times of the graphene-Bi_2Te_3 heterostructure open opportunities for applications such as in pulse lasers and optical switching.

To produce the graphene-Bi_2Te_3 heterostructure, we used two-step chemical vapour deposition (CVD). The monolayer graphene was grown on copper foils (thickness 25 μm; Alfa Aesar, item no. 13382).[32] Bi_2Te_3 powder (purity: 99.999%) was purchased from Alfa Aesar. Physical vapour deposition was used to produce the Bi_2Te_3 nanoplatelets on the graphene substrate. The detailed synthesis process of graphene-Bi_2Te_3 heterostructure can be found in our previous work.[31] In contrast to mechanically overlapping Bi_2Te_3 with graphene, the two-step CVD method can form van der Waals interactions between the monolayer graphene and Bi_2Te_3 nanoplatelet materials. The morphology of the graphene-Bi_2Te_3 heterostructure was investigated by scanning electron microscopy (SEM, FEI Quanta 200 FEG, acceleration voltage: 5–30 kV). Atomic force microscopy (AFM) was used to study the thickness and morphology of the graphene-Bi_2Te_3 heterostructure (Veeco Dimension-Icon). Raman spectroscopy was performed on a confocal micro-Raman system (Horiba Jobin-Yvon Labram HR800). The optical transmission spectra of a black phosphorus (BP) suspension were characterized by a UV-visible-IR spectrophotometer.

The ultrafast dynamical response measurements were performed using a femtosecond pulse laser with pulse duration of 35 fs. The femtosecond laser pulse was produced by an optical parametric amplifier (TOPAS, USF-UV2), which was pumped by a Ti:sapphire regenerative amplifier system (Spectra-Physics, Spitfire ACE-35F-2KXP Maitai SP and Empower 30). The pulse repetition rate was 2 kHz. The laser beam was focused by a lens with a focus distance of 250 mm. Both the pump light and the probe light were 1550 nm. The ultrafast dynamic relaxation process was measured by a pump-probe experimental system. The open-aperture (OA) and closed-aperture (CA) Z-scan experiments were performed at 1550 nm. The laser beam was focused by a lens with a focus distance of 150 mm.

Fig. 1(a) shows a typical SEM image of the graphene-Bi_2Te_3 heterostructure. Bi_2Te_3 nanoplatelets grew on top of the graphene film with a coverage of 20%, which can be controlled by the growth time during the CVD process. The lateral size of nanoplatelets is varied from 300 nm to 1.6 μm. Considering the similar hexagonal crystal structure, small lattice mismatch (~2.7%), and similar thermal expansion coefficient of graphene and Bi_2Te_3, a well-defined van der Waals interface was assumed to form between graphene and Bi_2Te_3. The as-grown Bi_2Te_3 nanoplatelets have an average thickness of 8.5 nm, as measured from the AFM topography images in Fig. 1(b).

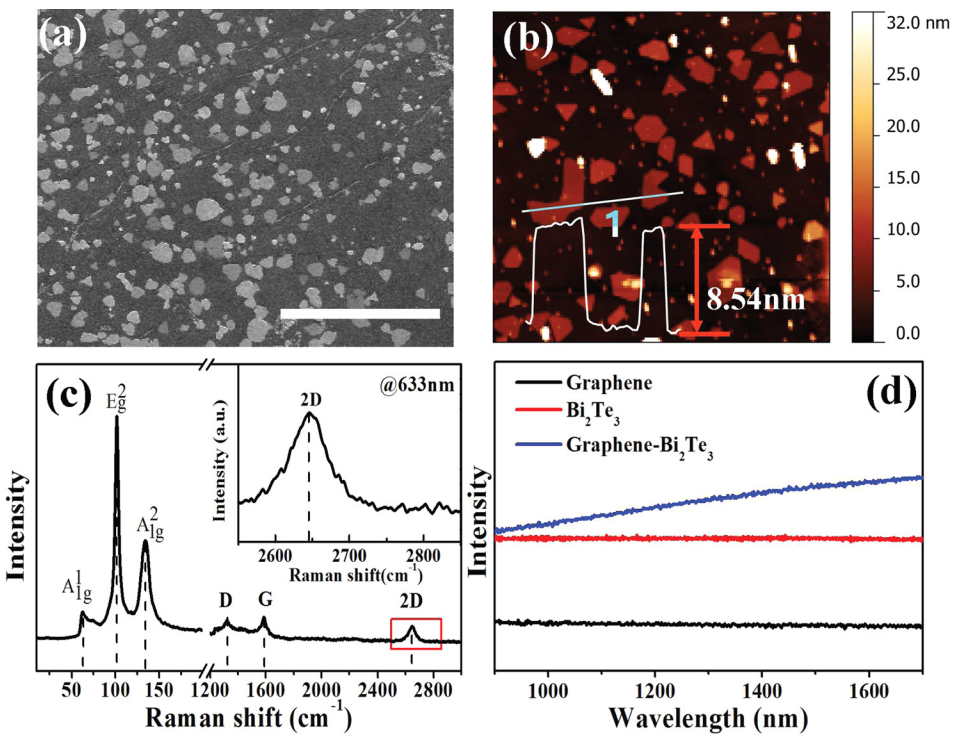

FIG. 1. Material characterization of the graphene-Bi_2Te_3 heterostructure. (a) SEM image of the graphene-Bi_2Te_3 heterostructure. Scale bar: 10 μm. (b) AFM image of the graphene-Bi_2Te_3 heterostructure. (c) Raman spectrum of the graphene-Bi_2Te_3 heterostructure; Inset: magnified view of the region marked by the red square in the Raman spectrum. (d) Near-IR absorption spectra of pure graphene, pure Bi_2Te_3 and graphene-Bi_2Te_3 heterostructure.

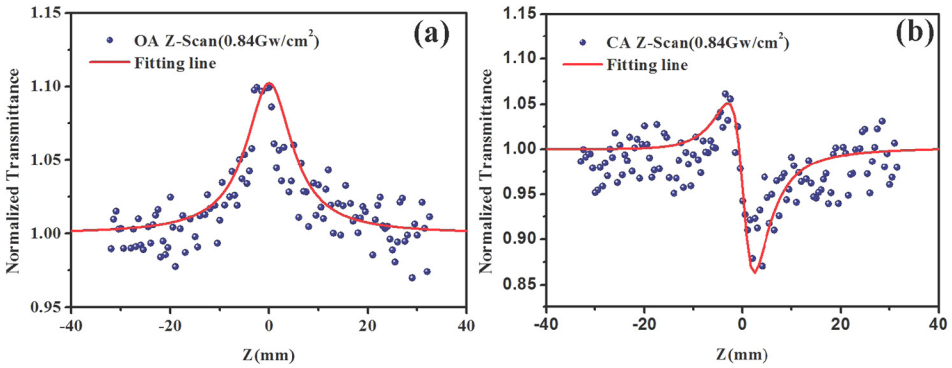

FIG. 2. Z-scan measurements of the graphene-Bi_2Te_3 heterostructure (a) OA Z-scans and (b) CA Z-scans measured with a 2-kHz laser pulse repetition rate at the same excitation irradiances; the red line shows the fitting result.

Fig. 1(c) shows the Raman spectrum of the graphene-Bi_2Te_3 heterostructure at 633 nm laser excitation. Two typical Raman active modes, the G-band and 2D-band, are observed at 1586 cm^{-1} and 2645 cm^{-1}, respectively, corresponding to the stretching of the C-C bond and a second-order, two-phonon process in the sp^2 carbon systems. The 2D-band is located at approximately 2645 cm^{-1} with a symmetric peak, indicating the monolayer nature of the graphene film in the heterostructure,[33] as shown in the inset of Fig. 1(c). In the low-frequency region, three characteristic peaks occur at 61.8 cm^{-1}, 101.4 cm^{-1}, and 134.0 cm^{-1}, corresponding to the three typical Raman active modes A_{1g}^1, E_g^1, and A_{1g}^2 in Bi_2Te_3, respectively. The typical linear optical absorption spectra of the graphene-Bi_2Te_3 heterostructure (and those of pure graphene and pure Bi_2Te_3 as references) are depicted in Fig. 1(d). The linear optical absorption of the heterostructure is markedly higher than those of the control samples in the near-IR range from 1000 to 1800 nm, which covers all the telecommunication bands. These results unambiguously reveal that Bi_2Te_3 imbues the heterostructure with strong broadband light absorption.

The Z-scan measurements were collected to determine the nonlinear refraction and absorption corresponding to the real and imaginary parts of the refractive index of the Kerr-type nonlinearity. During the OA Z-scan measurement, all the light transmitted through the sample was collected by a photodetector. For the CA Z-scan measurement, only the on-axis portion of the diffracted beam was collected. Fig. 2 illustrates the typical OA Z-scan traces and CA Z-scan traces at 1550 nm with a peak intensity of 0.84 GW/cm^2.

By assuming a spatially and temporally Gaussian profile for incoming laser pulses, the normalized energy transmittance $T_{OA}(z)$ can be given by[34–36]

$$T_{OA}(z) = \frac{1}{\sqrt{\pi} q_0} \int_{-\infty}^{\infty} \ln\left[L + q_0 \exp(-x^2)\right] dx, \qquad (1)$$

where $q_0 = \alpha_{NL} I_0 L_{\text{eff}}$, α_{NL} is the nonlinear optical absorption coefficient, $L_{eff} = [1 - \exp(-\alpha L)]/\alpha$, α is the linear absorption coefficient, and L is the sample path length.

The nonlinear optical absorption coefficient α_{NL} can be extracted by fitting the above equation to the OA Z-scan curves. For the OA Z-scan in Fig. 2(a), the best fit resulting in a nonlinear absorption coefficient is $\alpha_{NL} = -15 \times 10^{-4}$ cm/W for the graphene-Bi_2Te_3 heterostructure. Based on the best fit and the Z-scan theoretical solution,[37] the values of the nonlinear refraction coefficient n_2 can be determined to be approximately $n_2 = 0.2 \times 10^{-7}$ cm^2/W. Table I summarizes the nonlinear refractive indexes of different materials, i.e., graphene, Si, GaAs, Bi_2Se_3, and graphene-Bi_2Te_3 in present work. The graphene-Bi_2Te_3 heterostructure possesses a remarkably large nonlinear refractive index compared to other 2D and traditional bulk materials. The outstanding nonlinear response of nonlinear refractive indicates that the graphene-Bi_2Te_3 heterostructures show a tempting potential application in optical switching, mode-locking at telecommunication wavelengths.

In photoelectronic applications, alternative materials' carrier dynamics are key characteristics for the performance of devices. Graphene, which is an excellent nonlinear optical material, was used to produce a saturable absorber. Graphene has an ultrafast intraband electron relaxation time ($\tau_1 \approx 100$ fs) and interband electron relaxation time ($\tau_2 = 1.5$ ps).[13,45] For Bi_2Te_3, τ_1 and τ_2 exceed 500 fs and 5 ps,[28] respectively. Fig. 3 presents the carrier dynamics relaxation process for the graphene-Bi_2Te_3 heterostructure obtained at pump and probe wavelengths of 1550 nm with a pump incident intensity of 0.84 GW/cm^2. Based on the best fit with the biexponential decay theoretical solution ($y = A_1 \exp(-t/\tau_1) + A_2 \exp(-t/\tau_2)$), the values of τ_1 and τ_2 can be extracted from the pump-probe data as 270 ± 20 fs and 3.6 ± 0.2 ps, respectively. Considering the dynamic relaxation theory,[12] τ_1 and τ_2 are correlated with the intraband dynamic relaxation and interband carrier recombination. The energy band diagram of graphene-Bi_2Te_3 heterostructure is shown inset of Fig. 3. A relatively fast relaxation time compared to that of the pure Bi_2Te_3, which is an accelerated relaxation process, can be seen. Thus, the effect of the interface between graphene and Bi_2Te_3 significantly affected the

TABLE I. Nonlinear refractive index n_2 and nonlinear absorption α_{NL} of different materials.

Material	Wavelength (nm)	n_2 (cm^2/W)	α_{NL} (cm/W)
Graphene	1550	10^{-7}[a]	$\sim 10^{-8}$[b]
Si	1550	$\sim 10^{-14}$[c]	…
GaAs	1540	10^{-13}[d]	…
Bi_2Se_3	800	2.26×10^{-10}[e]	…
Bi_2Te_3	1550	$\sim 10^{-8}$[f]	$\sim 10^{-5}$[g]
Graphene-Bi_2Te_3	1550	0.2×10^{-7}[g]	-15×10^{-4}[g]

[a]References 10 and 38.
[b]Reference 44.
[c]Reference 39.
[d]References 40 and 41.
[e]Reference 42.
[f]Reference 43.
[g]Present work.

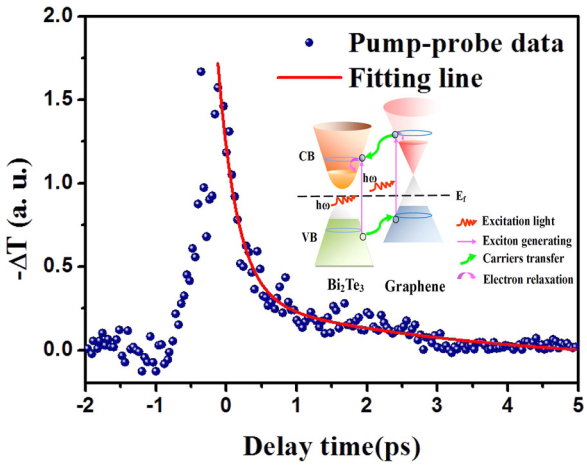

FIG. 3. Pump-probe signals measured as a function of the delay time at 1550 nm; the red line shows the fitting result. Inset: schematic diagram showing the carrier transfer in the graphene−Bi_2Te_3 heterostructure.

dynamic relaxation process of the photoexcited carriers. Herein, the graphene-Bi_2Te_3 heterostructures were transferred onto transparent quartz, which possesses a bandgap several times than that of the pump(probe) photon energy. Thus, the substrate did not contribute to the pump-probe signal.

Based on the covalent donor-acceptor structure,[6,31,46,47] we explain the dynamic relaxation process in the graphene-Bi_2Te_3 heterostructure. An energy diagram is shown inset of Fig. 3. From previous works,[48] we know that graphene possesses a P-type doping state because of the existence of substrates, defects, water molecules, and oxygen in the air. Additionally, the Bi_2Te_3 possesses an N-type bulk state because of Te vacancies.[49,50] The work function of Bi_2Te_3 ($\sim$5.3 eV)[51] is higher than that of graphene ($\sim$4.6 eV).[52] Given the different doping types of graphene and Bi_2Te_3, a typical metal-semiconductor contact forms at their interface. Therefore, the graphene acts as an electron donor through covalent interactions between graphene and Bi_2Te_3. When photoexcited electrons are generated in graphene by pump light excitation, they move into the conduction band of Bi_2Te_3. Subsequently, they enter the Bi_2Te_3, and photoexcited holes move to the valence band of graphene. Thus, photoexcited electrons rapidly accumulate in the conduction band of Bi_2Te_3, which may accelerate the photoexcited electron dynamic relaxation and intraband and photoexcited carrier interband recombination. In contrast, the transfer of photoexcited carriers between graphene and Bi_2Te_3 effectively suppresses the photogenerated electron dynamic intraband relaxation and recombination of photogenerated carriers in graphene. As a result, a relatively fast relaxation time is observed in the graphene-Bi_2Te_3 heterostructure compared to that in pure Bi_2Te_3.

In conclusions, we report a large nonlinear refraction and ultrafast dynamic relaxation time of the graphene-Bi_2Te_3 heterostructure. By combining the unique properties of graphene and Bi_2Te_3, we obtained a nonlinear refractive index of $n_2 = 0.2 \times 10^{-7}$ cm^2/W and an ultrafast dynamic relaxation time (intraband relaxation time $\tau_1 = 270 \pm 20$ fs; interband relaxation time $\tau_2 = 3.6 \pm 0.2$ ps) in the heterostructure. The results prove that the graphene-Bi_2Te_3 heterostructure possesses remarkable nonlinear optical properties and exhibits a fascinating dynamic response. A carrier transfer model is proposed based on the donor-acceptor structure model to understand the relaxation dynamics mechanism in the graphene-Bi_2Te_3 heterostructure. We anticipated that the unique nonlinear optical and ultrafast dynamic characteristics of the graphene-Bi_2Te_3 heterostructure may lead to significant applications in pulse lasers and optical switching.

The authors gratefully acknowledge the support from the National Natural Science Foundation of China (Grant No. 61222406, 11174371, 11404410, 51272291, 51222208, 51290273, and 91433107), the 863 Program (Grant No. 2013AA031903), the youth 973 program (2015CB932700), Hunan Provincial Natural Science Foundation of China (12JJ1001), the Specialized Research Fund for the Doctoral Program of Higher Education (20110162120072), and Undergraduate Training Program for Innovation and Entrepreneurship of Central South University (201510533248), the Fundamental Research Funds for the Central Universities of Central South University (2016zzts016 and 2016zzts225).

[1]A. K. Geim and K. S. Novoselov, Nat. Mater. **6**, 183 (2007).
[2]K. S. Novoselov and A. A. Firsov, Science **306**, 666 (2004).
[3]B. Radisavljevic, M. B. Whitwick, and A. Kis, Appl. Phys. Lett. **101**, 043103 (2012).
[4]D. Sarkar, W. Liu, X. Xie, A. Anselmo, S. Mitragotri, and K. Banerjee, ACS Nano **8**, 3992 (2014).
[5]H. Zhang, D. Y. Tang, L. M. Zhao, Q. L. Bao, and K. P. Loh, Opt. Commun. **283**, 3334 (2010).
[6]H. R. Mu, Z. T. Wang, J. Yuan, S. Xiao, C. Y. Chen, Y. Chen, Y. Chen, J. C. Song, Y. S. Wang, Y. Z. Xue, H. Zhang, and Q. L. Bao, ACS Photonics **2**, 832 (2015).
[7]Y. Chen, G. Jiang, S. Chen, Z. Guo, X. Yu, C. Zhao, H. Zhang, Q. Bao, S. Wen, D. Tang, and D. Fan, Opt. Express **23**, 12823 (2015).
[8]S. B. Lu, L. L. Miao, Z. N. Guo, X. Qi, C. J. Zhao, H. Zhang, S. C. Wen, D. Y. Tang, and D. Y. Fan, Opt. Express **23**, 11183 (2015).
[9]Y. W. Wang, G. H. Huang, H. R. Mu, S. H. Lin, J. Z. Chen, S. Xiao, Q. L. Bao, and J. He, Appl. Phys. Lett. **107**, 091905 (2015).
[10]J. Zhang, X. Yu, W. Han, B. Lv, X. Li, S. Xiao, Y. Gao, and J. He, Opt. Lett. **41**, 1704 (2016).
[11]H. Zhang, V. Stephane, Q. L. Bao, K. P. Loh, M. Serge, G. Nicolas, and K. Pascal, Opt. Lett. **37**, 1856 (2012).
[12]P. A. George, J. Strait, J. Dawlaty, S. Shivaraman, M. Chandrashekhar, F. Rana, and M. G. Spencer, Nano Lett. **8**, 4248 (2008).
[13]Q. L. Bao and K. P. Loh, ACS Nano **6**, 3677 (2012).
[14]Y. H. Lin, C. Y. Yang, J. H. Liou, C. P. Yu, and G. R. Lin, Opt. Express **21**, 16763 (2013).
[15]Q. W. Sheng, M. Feng, W. Xin, H. Guo, T. Y. Han, Y. G. Li, Y. G. Liu, F. Gao, F. Song, and Z. B. Liu, Appl. Phys. Lett. **105**, 041901 (2014).
[16]T. Feng, S. Zhao, K. Yang, G. Li, D. Li, J. Zhao, W. Qiao, J. Hou, Y. Yang, and J. He, Opt. Express **21**, 24665 (2013).
[17]R. Mary, G. Brown, S. J. Beecher, F. Torrisi, S. Milana, D. Popa, T. Hasan, Z. Sun, E. Lidorikis, S. Ohara, A. C. Ferrari, and A. K. Kar, Opt. Express **21**, 7943 (2013).
[18]A. Martinez and Z. P. Sun, Nat. Photonics **7**, 842 (2013).
[19]X. L. Qi and S. C. Zhang, Rev. Mod. Phys. **83**, 1057 (2011).
[20]M. Z. Hasan and C. L. Kane, Rev. Mod. Phys. **82**, 3045 (2010).
[21]C. Zhao, Y. Zou, Y. Chen, Z. Wang, S. Lu, H. Zhang, S. Wen, and D. Tang, Opt. Express **20**, 27888 (2012).
[22]C. Zhao, H. Zhang, X. Qi, Y. Chen, Z. Wang, S. Wen, and D. Tang, Appl. Phys. Lett. **101**, 211106 (2012).
[23]Z. Luo, Y. Huang, J. Weng, H. Cheng, Z. Lin, B. Xu, Z. Cai, and H. Xu, Opt. Express **21**, 29516 (2013).
[24]P. Tang, X. Zhang, C. Zhao, Y. Wang, H. Zhang, D. Shen, S. Wen, D. Tang, and D. Fan, IEEE. Photonics J. **5**, 1500707 (2013).
[25]Y. Chen, M. Wu, P. Tang, S. Chen, J. Du, G. Jiang, Y. Li, C. Zhao, H. Zhang, and S. Wen, Laser Phys. Lett. **11**, 055101 (2014).
[26]Y. H. Lin, C. Y. Yang, S. F. Lin, W. H. Tseng, Q. Bao, C. I. Wu, and G. R. Lin, Laser Phys. Lett. **11**, 055107 (2014).

[27]S. Q. Chen, C. J. Zhao, Y. Li, H. H. Huang, S. B. Lu, H. Zhang, and S. C. Wen, Opt. Mater. Express **4**, 587 (2014).
[28]M. Hajlaoui, E. Papalazarou, J. Mauchain, G. Lantz, N. Moisan, D. Boschetto, Z. Jiang, I. Miotkowski, Y. Chen, and A. Taleb-Ibrahimi, Nano Lett. **12**, 3532 (2012).
[29]M. Hajlaoui, E. Papalazarou, J. Mauchain, Z. Jiang, I. Miotkowski, Y. P. Chen, A. Taleb-Ibrahimi, L. Perfetti, and M. Marsi, Eur. Phys. J. Spec. Top. **222**, 1271 (2013).
[30]B. Liang, Z. J. Song, M. H. Wang, L. J. Wang, and W. Jiang, J. Nanomater. **2013**, 210767.
[31]H. Qiao, J. Yuan, Z. Q. Xu, C. Y. Chen, S. H. Lin, Y. S. Wang, J. C. Song, Y. Liu, Q. Khan, H. Y. Hoh, C. X. Pan, S. J. Li, and Q. L. Bao, ACS Nano **9**, 1886 (2015).
[32]X. Li, W. Cai, J. An, S. Kim, J. Nah, D. Yang, R. Piner, A. Velamakanni, I. Jung, and E. Tutuc, Science **324**, 1312 (2009).
[33]A. C. Ferrari, J. C. Meyer, V. Scardaci, C. Casiraghi, M. Lazzeri, F. Mauri, S. Piscanec, D. Jiang, K. S. Novoselov, S. Roth, and A. K. Geim, Phys. Rev. Lett. **97**, 187401 (2006).
[34]R. L. Sutherland, *Handbook of Nonlinear Optics* (Marcel Dekker, New York, 2003).
[35]B. Gu, D. H. Liu, J. L. Wu, J. He, and Y. P. Cui, Appl. Phys. B **117**, 1141 (2014).
[36]Y. Q. Wang, J. He, S. Xiao, N. A. Yang, and H. Z. Chen, Acta Phys. Sin. **63**, 144204 (2014).
[37]J. He, Y. L. Qu, H. P. Li, J. Mi, and W. Ji, Opt. Express **13**, 9235 (2005).
[38]E. Hendry, P. Hale, J. Moger, A. Savchenko, and S. Mikhailov, Phys. Rev. Lett. **105**, 97401 (2010).
[39]X. Wang, Z. Shen, J. Lu, and X. Ni, J. Appl. Phys. **108**, 033103 (2010).
[40]M. Dinu, F. Quochi, and H. Garcia, Appl. Phys. Lett. **82**, 2954 (2003).
[41]A. Garg, A. Kapoor, and K. Tripathi, Opt. Laser Technol. **35**, 21 (2003).
[42]S. B. Lu, C. J. Zhao, Y. H. Zou, S. Q. Chen, Y. Chen, Y. Li, H. Zhang, S. C. Wen, and D. Y. Tang, Opt. Express **21**, 2072 (2013).
[43]B. Shi, L. Miao, Q. Wang, J. Du, P. Tang, J. Liu, C. Zhao, and S. Wen, Appl. Phys. Lett. **107**, 151101 (2015).
[44]S. Kumar, M. Anija, N. Kamaraju, K. S. Vasu, K. S. Subrahmanyam, A. K. Sood, and C. N. R. Rao, Appl. Phys. Lett. **95**, 191911 (2009).
[45]Q. L. Bao, H. Zhang, Z. Ni, Y. Wang, L. Polavarapu, Z. Shen, Q. H. Xu, D. Tang, and K. P. Loh, Nano Res. **4**, 297 (2011).
[46]Y. F. Xu, Z. B. Liu, X. L. Zhang, Y. Wang, J. G. Tian, Y. Huang, Y. F. Ma, X. Y. Zhang, and Y. S. Chen, Adv. Mater. **21**, 1275 (2009).
[47]C. N. R. Rao, A. K. Sood, R. Voggu, and K. S. Subrahmanyam, J. Phys. Chem. Lett. **1**, 572 (2010).
[48]Y. Shi, W. Fang, K. Zhang, W. Zhang, and L. J. Li, Small **5**, 2005 (2009).
[49]J. W. G. Bos, H. W. Zandbergen, M. H. Lee, N. P. Ong, and R. J. Cava, Phys. Rev. B **75**, 195203 (2007).
[50]Y. Chen, J. Analytis, J. H. Chu, Z. Liu, S. K. Mo, X. L. Qi, H. Zhang, D. Lu, X. Dai, and Z. Fang, Science **325**, 178 (2009).
[51]M. Chen, J. P. Peng, H. M. Zhang, L. L. Wang, K. He, X. C. Ma, and Q. K. Xue, Appl. Phys. Lett. **101**, 081603 (2012).
[52]Y. J. Yu, Y. Zhao, S. Ryu, L. E. Brus, K. S. Kim, and P. Kim, Nano Lett. **9**, 3430 (2009).